AMERICAN ACADEMY OF OPHTHALMOLOGY®

Application of Automated Quantification of Fluid Volumes to Anti–VEGF Therapy of Neovascular Age-Related Macular Degeneration

Ursula Schmidt-Erfurth, MD,[1] *Wolf-Dieter Vogl, PhD,*[1] *Lee Merrill Jampol, MD,*[2] *Hrvoje Bogunović, PhD*[1]

Purpose: Anti–vascular endothelial growth factor (VEGF) treatment of neovascular age-related macular degeneration (AMD) is a highly effective advance in the retinal armentarium. OCT offering 3-dimensional imaging of the retina is widely used to guide treatment. Although poor outcomes reported from clinical practice are multifactorial, availability of reliable, reproducible, and quantitative evaluation tools to accurately measure the fluid response, that is, a "VEGF meter," may be a better means of monitoring and treating than the current purely qualitative evaluation used in clinical practice.

Design: Post hoc analysis of a phase III, randomized, multicenter study.

Participants: Study eyes of 1095 treatment-naive subjects receiving pro re nata (PRN) or monthly ranibizumab therapy according to protocol-specified criteria in the HARBOR study.

Methods: A deep learning method for localization and quantification of fluid in all retinal compartments was applied for automated segmentation of fluid with every voxel classified by a convolutional neural network (CNN). Three-dimensional volumes (nanoliters) for intraretinal fluid (IRF), subretinal fluid (SRF), and pigment epithelial detachment (PED) were determined in 24 362 volume scans obtained from 1095 patients treated over 24 months in a phase III clinical trial with randomization to 2 drug dosages (0.5 mg and 2.0 mg ranibizumab) and 2 regimens (monthly and PRN). A multivariable mixed-effects regression model was used to test for differences in fluid between the arms and for fluid/function correlation.

Main Outcome Measures: Fluid volume in nanoliters, structure-function as Pearson's correlation coefficient, and as a coefficient of determination (R^2).

Results: Fluid volumes were quantified in all visits of all patients. Automated segmentation demonstrated characteristic response patterns for each fluid compartment individually: Intraretinal fluid showed the greatest and most rapid resolution, followed by SRF and PED the least. The loading dose treatment achieved resolution of all fluid types close to the lowest levels attainable. Dosage and regimen parameters correlated directly with resulting fluid volumes. Fluid/function correlation showed a volume-dependent negative impact of IRF on vision and weak positive prognostic effect of SRF.

Conclusions: Automated quantification of the fluid response may improve therapeutic management of neovascular AMD, avoid discrepancies between clinicians/investigators, and establish structure/function correlations. *Ophthalmology 2020;127:1211-1219 © 2020 by the American Academy of Ophthalmology. This is an open access article under the CC BY-NC-ND license (http://creativecommons.org/licenses/by-nc-nd/4.0/).*

Supplemental material available at www.aaojournal.org.

Worldwide severe vision loss increased by 24% between 2005 and 2015.[1] Exudative age-related macular degeneration (AMD) is a major threat to central vision.[2] Pathological macular neovascularization can destroy the retinal pigment epithelium (RPE) and neurosensory retina.[3] Neovascular leakage allows fluid to accumulate in the macula manifesting as intraretinal fluid (IRF) or fluid pooling underneath the retina as subretinal fluid (SRF) or pigment epithelial detachment (PED). Fluid in these compartments compromises best-corrected visual acuity (BCVA) to variable degrees. By 2 years, in half of the eyes, fluid results in irreversible fibrotic scarring.[4] Inhibition of vascular endothelial growth factor (VEGF) by intravitreal injection of antibodies was the first treatment to achieve meaningful stabilization or improvement of visual acuity with a decrease in fluid. Anti-VEGF treatment is considered a major breakthrough in the management of neovascular AMD.[5] Currently, intravitreal therapy is the most frequent intervention in ophthalmology and results in a substantial socioeconomic benefit.

https://doi.org/10.1016/j.ophtha.2020.03.010
ISSN 0161-6420/20

Advances in diagnostic imaging have also emerged with high-resolution 3-dimensional OCT. The ability of spectral-domain (SD) OCT to visualize the macular anatomy and abnormal fluid in the retinal compartments has led to widespread adoption of OCT imaging. More than 30 million OCT procedures with an estimated cost of 1 billion USD per year are currently performed in the United States alone.[6] Pivotal trials have assessed the presence of fluid on OCT using excess central retinal thickness (CRT) as the major guide for treatment decisions.[7,8] However, correlations of CRT with BCVA have been disappointing.[9] The qualitative identification of fluid is prone to errors with frequent discrepancies between physicians' decisions and certified reading center evaluations. This has resulted in a substantial number of missed treatments even in clinical trials.[8] The inability to reliably identify, localize, and quantify fluid in OCT scans results in a variability in injection rates, reimbursement expenses, and unsatisfactory clinical outcomes in the real world.[10]

The introduction of artificial intelligence (AI) has great promise for tackling many diagnostic and therapeutic challenges in medicine.[11] Large OCT volumes in the range of 60 to 100 million voxels per image are particularly amenable to AI-based segmentation of physiologic and pathological features, identification of disease-related patterns, determination of therapeutic efficacy, and structure/function correlation in a rapid and reproducible manner.[12] Our group previously designed an algorithm for fully automated detection and quantification of macular fluid using deep learning.[13] In this article, we evaluate the clinical concept of AI-based fluid quantification in one of the most comprehensive imaging data sets available, the HARBOR trial.

Methods

Participants

Artificial intelligence–based analysis was performed on SD-OCT scans of 1095 patients enrolled in the HARBOR trial (ClinicalTrials.gov identifier: NCT00891735). HARBOR was a 24-month, phase III, randomized, multicenter study to evaluate the efficacy and safety of intravitreal ranibizumab at 2 dosages (0.5 mg and 2.0 mg) and 2 regimens: fixed monthly and flexible pro re nata (PRN) in treatment-naïve patients with subfoveal neovascular AMD[14] (Fig 1). Patients in the PRN groups underwent monthly evaluations and received ranibizumab monthly for the first 3 doses. Subsequently, they received ranibizumab only if the re-treatment criteria were met (a ≥5-letter decrease in BCVA or any evidence of disease activity on OCT). The BCVA was measured at each visit using Early Treatment Diabetic Retinopathy Study charts. Retinal scans were acquired following a standardized protocol using a CIRRUS HD-OCT III (Carl Zeiss Meditec, Inc, Dublin, CA) consisting of $512 \times 128 \times 1024$ voxels with the size of $11.7 \times 47.2 \times 2.0$ μm^3, comprising a volume of $6 \times 6 \times 2$ mm^3. This post hoc analysis was conducted in compliance with the Declaration of Helsinki, and approval was obtained by the Ethics Committee at the Medical University of Vienna (EK Nr: 1246/2016). All participants provided informed consent at the respective centers before enrollment into the HARBOR clinical trial.

Automated Fluid Localization and Quantification

Automated 3-dimensional OCT segmentation of the 3 fluid types (Fig 2) was performed on all of the 24 362 available volume scans. A deep learning method for IRF and SRF segmentation was developed as proprietary intellectual property of the Medical University of Vienna and trained and validated as shown previously.[13] Every voxel was classified with a multi-scale convolutional neural network (CNN) and assigned to 1 of the 4 classes: background, retina, IRF, or SRF. Further evaluation of the CNN by comparing the automated fluid volume measurements with those obtained from manual annotations is provided in Figures S1 and S2 and Videos 1-4 (available at www.aaojournal.org). Pigment epithelial detachment was identified by segmenting the region between RPE and Bruch's membrane, which was delineated using an automated graph-theoretic method, part of the Iowa Reference Algorithms.[15,16] Any segmented region was considered as PED if it had a height >200 μm or width >400 μm, as originally defined by the Vienna, Duke, and Wisconsin reading centers.[17-19] If a voxel gets classified as both PED and SRF, the SRF class was used because the CNN output was expected to be more accurate. Absolute volumes (1 nl = 0.001 mm^3) of IRF, SRF, and PED were computed within the central 1-mm and central 6-mm cylinders around the fovea.

Statistical Analysis and the Correlation of Fluid and Function

To test for differences in fluid volumes across treatment arms at the end of the trial, a nonparametric Mann–Whitney U test was performed, because fluid volume distributions were skewed toward zero value. Structure–function correlation is reported as Pearson's r coefficient. To obtain a population mean response to therapy, the trajectory of BCVA over time was modeled with a piecewise linear function as a multivariable repeated-measure mixed-effects regression model including fluid volumes as covariates.[20] Best-corrected visual acuity was the outcome variable, time and fluid volume covariates were fixed effects, and individually varying intercept and slope were modeled as random effects. To model the rapid changes in BCVA and fluid volume after the first treatment, we used a piecewise linear model with the split-point at the first follow-up visit. All parameters were determined by restricted maximum likelihood. Residual plots were used to validate the models' assumptions. Goodness-of-fit was measured using coefficient of determination (R^2) for mixed-effects models[21] that consists of marginal R^2 considering variance explained by fixed effects only and conditional R^2 considering both fixed and random effects. The 95% confidence intervals were obtained by bootstrap sampling with 500 simulations. P values and t statistics were calculated on the basis of Satterthwaite's approximations. All computation was performed on R (Version 3.4.2, The R Project For Statistical Computing, Vienna, Austria) using lme4 package (Version 1.1.18.1).[22]

Role of the Funding Source

The sponsor of the study (the Austrian Federal Ministry for Digital and Economic Affairs) had no role in data collection, data analysis, data interpretation, or writing of the report. The corresponding author had full access to the data and

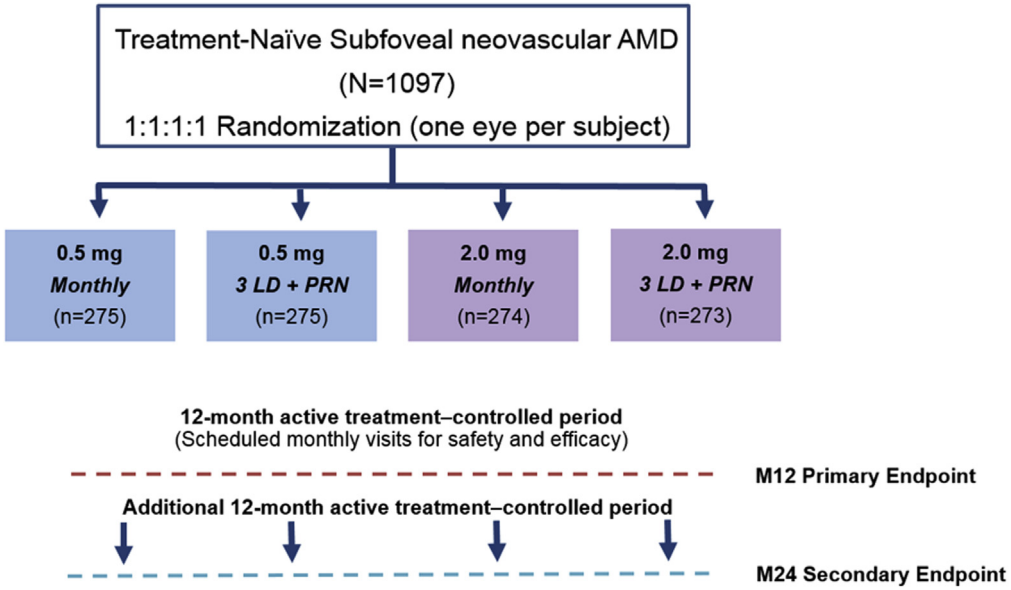

Figure 1. Randomization regarding drug dose and regimen across the 4 treatment arms in the prospective HARBOR phase III clinical trial. Patients with treatment—naïve neovascular age-related macular degeneration (AMD) received fixed monthly or flexible pro re nata (PRN) anti-vascular endothelial growth factor (VEGF) therapy using ranibizumab. All monthly visits included a standardized morphological OCT examination (CIRRUS) and best-corrected visual acuity (BCVA) functional test. LD = loading dose.

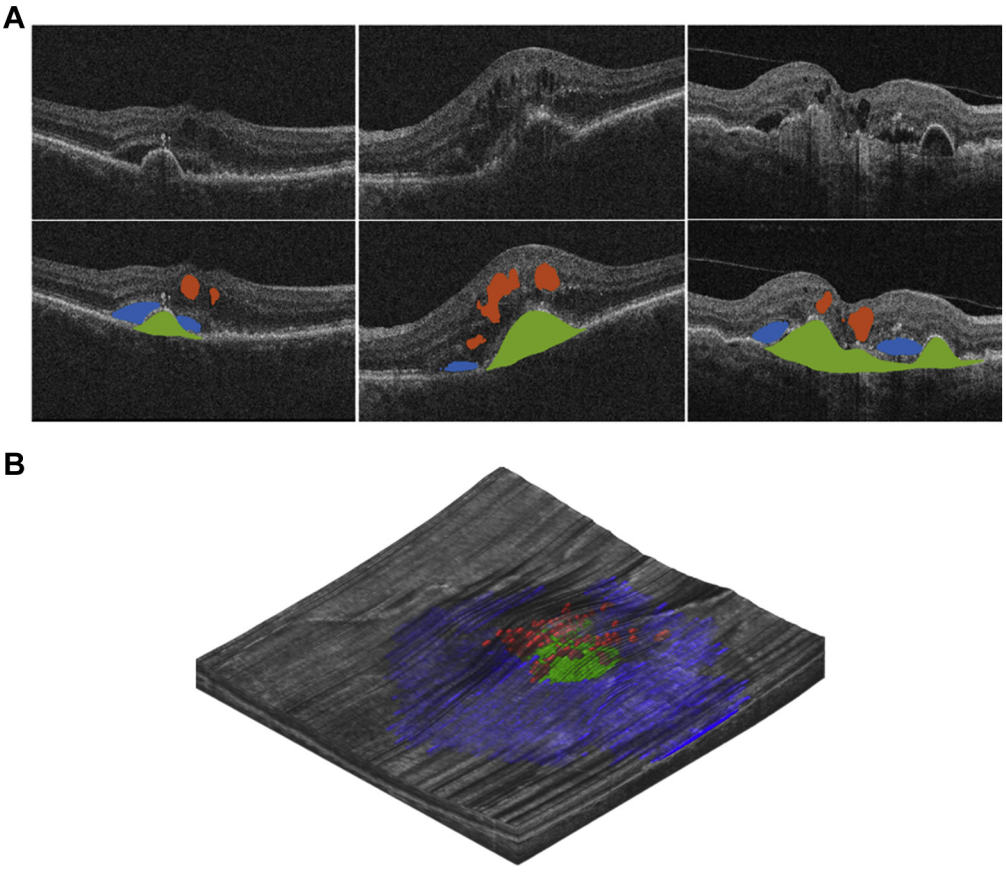

Figure 2. A, Representative examples of fully automated image segmentation of the 3 fluid compartments: intraretinal fluid (IRF) (in red), subretinal fluid (SRF) (in blue), and pigment epithelial detachment (PED) (in green). **B,** Fluid localization and quantification were performed in a 3-dimensional manner throughout the entire volume of each individual OCT data set.

final responsibility for the decision to submit for publication.

Results

Therapeutic Response by Compartment

Automated segmentation using deep learning allowed comprehensive measurement of fluid volumes at all visits. Patterns of fluid resolution in the central 6 mm were noted (Fig 3A): Intraretinal fluid resolved rapidly after the first injection and remained low over 24 months of follow-up. The mean volume of SRF at baseline was 3 times larger than that of IRF. The first injection resulted in substantial SRF resolution, and SRF pooling remained low subsequently. By contrast, PED showed a less pronounced reduction with no further resolution with continued treatment.

Fluid Resolution by Regimen

Quantitatively, the therapeutic response of the 2 IRF arms was similar with low residual IRF independent of fixed/flexible regimen. By contrast, the mean SRF volume in the monthly arm was less than in the PRN-treated arm. The differentiation by regimen was even more pronounced for PED, which resolved more intensively during a monthly re-treatment than by PRN (Fig 3B). Our values can be expressed in nanoliters (Fig 3C) and reflect the stability of measurements over time.

Therapeutic Effect on Foveal Fluid Volumes

Best-corrected visual acuity is mostly determined by foveal IRF and SRF. Therefore, central 1-mm volumes were analyzed separately by drug dose and regimen (Fig 4A, B). After a steep decline following the first treatment, the arms with the most intensive treatment (2.0 mg and monthly dosing) were always associated with the least residual fluid, whereas the arms with the least therapeutic effort (0.5 mg and flexible dosing) exhibited larger volumes of residual fluid. The values of IRF in the foveal mm were higher than for SRF, which was seen predominantly as extrafoveal extension.

At the end of the trial, in the central 1 mm, the monthly regimens for both dosages had significantly lower mean residual volumes compared with PRN, for IRF (difference of -0.55 nl, $P < 0.001$) and SRF (difference of -1.11 nl, $P = 0.031$). The 2.0 mg dose across regimens had significantly lower mean residual volumes compared with 0.5 mg, for IRF (difference of -1.86 nl, $P < 0.03$) and SRF (difference of -1.64 nl, $P = 0.02$).

Correlation of Fluid Location and Function

When fluid localization was correlated with visual function, a significant correlation was found between the neurosensory compartment and impact on BCVA (Fig 5A). Most of the correlation with vision was seen in the initial phase of the treatment. Subsequently, there is little fluid present and the variability in individual vision is associated with other retinal morphological changes. Although IRF consistently had a negative impact on vision, SRF correlated in a weak positive manner and PED resolution had little vision-modifying impact. These differences were maintained over all visits.

Correlation of Fluid Volume and Best-Corrected Visual Acuity

Per unit of 100 nl, an increase in IRF was found to be associated with a mean reduction in BCVA of -4.08 letters, whereas SRF was associated with a superior BCVA of $+1.99$ letters (Fig 5B). Both correlations were highly statistically significant. As the first injection led to a large reduction in IRF volumes, the change in BCVA due to the resolution of IRF alone correlated with a large initial increase in BCVA. With only small changes in IRF volumes during maintenance, the subsequent BCVA changes were small. Thus, there was no significant prognostic correlation (R^2 of 0.025) between fluid and function during extended follow-up.

Discussion

This study uses 3 recent advances in ophthalmology: diagnostic precision by SD-OCT imaging, therapeutic efficacy of anti-VEGF treatment, and potentially AI-based tools in search of an optimized disease management. Standardized structural monitoring using SD-OCT data obtained from an anti-VEGF study randomized regarding drug dose and re-treatment regimen were processed using a fully automated algorithm to measure fluid volumes in retinal compartments. We report that AI-based quantification of fluid volume offers a precise measurement of disease activity. This approach allows identification of response patterns and a correlation of fluid volumes with functional change. The resulting insights may improve the management of an individual patient as well as the care of large populations offering point-of-care in neovascular AMD.

OCT allows fast, noninvasive imaging with unprecedented in vivo resolution. The capacity of OCT to provide cross-sectional images of the macula allows localization of retinal fluid and provides advanced pathophysiologic insights into macular disease. Although conventional angiography provides only a 2-dimensional representation, 3-dimensional raster-scanning SD-OCT provides recognition of changes in various fluid compartments. It has been recognized as an excellent tool to monitor the anti-leakage effects of pharmacologic intervention, a "VEGF-meter."[23] Artificial intelligence–based quantification of these changes may advance the field by objectively and accurately monitoring the therapeutic responses.

The HARBOR trial[24] was the first phase III trial that implemented an OCT-guided flexible regimen offering the ability to introduce a deep learning algorithm based on a pixel level of tens of thousands of OCT scans. With our approach, we obtain accurate quantification of fluid volumes for all patients, visits, and dosages with insights into therapeutic response patterns.

The disappointing outcomes in current clinical practice are thought to be at least partially due to undertreatment.[25] Ophthalmologists are dealing with an increasing amount of imaging data. Re-treatments can easily be misjudged when qualitative assessments of an OCT fly-through series are made in a busy practice.[26] A real-world registry identified 27 974 patient visits of 46 specialists, where neovascular activity was rated "uncertain" for 72% of the providers resulting in potentially worse outcomes.[27] In CATT, fluid determined by investigators compared with reading center assessments showed absence of diagnostic discrepancies in only 20.9%.[28] With our approach, we

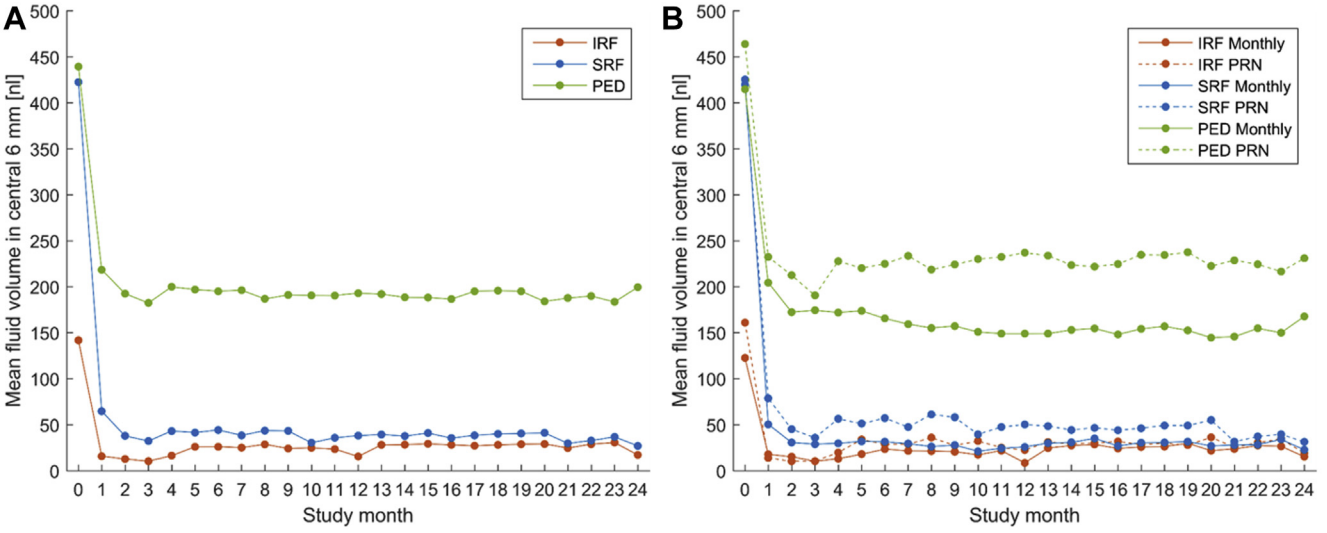

C

Month	0	1	2	3	4	5	6	7	8	9	10	11	12	13	14	15	16	17	18	19	20	21	22	23	24
IRF Monthly	123	18	15	10	13	18	23	22	21	21	17	22	9	25	27	29	24	26	26	30	22	24	27	27	15
IRF PRN	161	14	10	10	20	34	29	29	36	27	32	25	22	31	29	30	32	28	30	28	36	26	30	35	19
SRF Monthly	425	50	31	29	30	32	32	29	26	28	21	24	26	30	31	35	27	31	31	32	27	28	28	34	23
SRF PRN	420	79	45	36	56	51	57	48	61	58	40	47	50	49	44	47	44	46	49	49	55	32	37	40	31
PED Monthly	415	204	172	174	172	174	166	159	155	157	151	149	149	149	153	155	148	154	157	152	145	146	155	150	168
PED PRN	464	232	213	191	228	220	225	234	219	224	230	232	237	234	224	222	225	235	234	238	223	229	224	217	231

Figure 3. Response patterns by compartment indicating the mean fluid volumes within a 6 mm diameter over 24 months of anti-vascular endothelial growth factor (VEGF) treatment for intraretinal fluid (IRF) in red, subretinal fluid (SRF) in blue, and pigment epithelial detachment (PED) in green. Pooled by fluid type **(A)**, individually by regimen **(B)**, and numerically in nanoliters **(C)**. PRN = pro re nata.

demonstrate that pixel-wise fluid detection is achievable even at low nanoliter levels of retinal fluid.

Recently, CNNs were successfully trained on color photographs to screen for diabetic retinopathy.[29] Large 3-dimensional SD-OCT volumes are a bigger challenge for automated segmentation. We previously introduced a CNN that was able to learn to segment an image and identify the fluid components individually.[12] Accordingly, the evaluation (Supplementary material and Videos 1-4, available at www.aaojournal.org) performed on a comparable cohort of patients with neovascular AMD imaged with CIRRUS shows that the mean fluid volume values and limits of agreement are within the interobserver variability.

Intraretinal fluid has been recognized as an important hallmark of macular neovascularization. Experimental induction of IRF by VEGF exposure suggested that IRF was at least partially a retinal vascular consequence of focal VEGF release.[30] The diffuse pattern of multilocular pseudocysts in IRF is particularly difficult to assess quantitatively during clinical evaluation. However, IRF matters most for vision and worse BCVA was seen in eyes with greater baseline IRF,[31] as well as at year 1 in eyes with persistent IRF.[32] Intraretinal fluid volume and area both correlated directly with visual function when analyzed in a 3-dimensional manner.[33] By using AI-based tools, we are able to correlate the quantity of 3-dimensional fluid volumes (per unit of 100 nl) directly with BCVA change. Intraretinal fluid—related cystoid spaces resistant to even enhanced therapy in terms of dosage and frequency may represent neurosensory degeneration resulting in macular atrophy.[9] Our method identifies such persistent cystoid spaces even at low fluid levels.

Individual segmentation errors occur in OCT imaging of neovascular AMD. However, in this article, the analysis represents population-level values. Thus, even if an individual B-scan is poorly segmented, the population-level volume distributions are not expected to be affected.

In contrast to IRF, trials have shown SRF to be associated with superior baseline and outcome BCVA.[9,34] Subretinal fluid was associated with a lower risk for geographic atrophy,[35] which further highlights the need for reliable fluid localization. Because IRF and SRF appear spatially separated, with IRF seen foveally and SRF existing largely beyond the central 1 mm, the absolute amount of SRF is systematically underestimated.[36] The large volume of baseline SRF noted by quantitative AI was a surprise.

Pigment epithelial detachment—related fluid is most resistant to anti-VEGF treatment, and a higher dosage did not add functional benefit either in CATT, VIEW, or HARBOR.[8,24,37] Our AI-based analyses demonstrated no

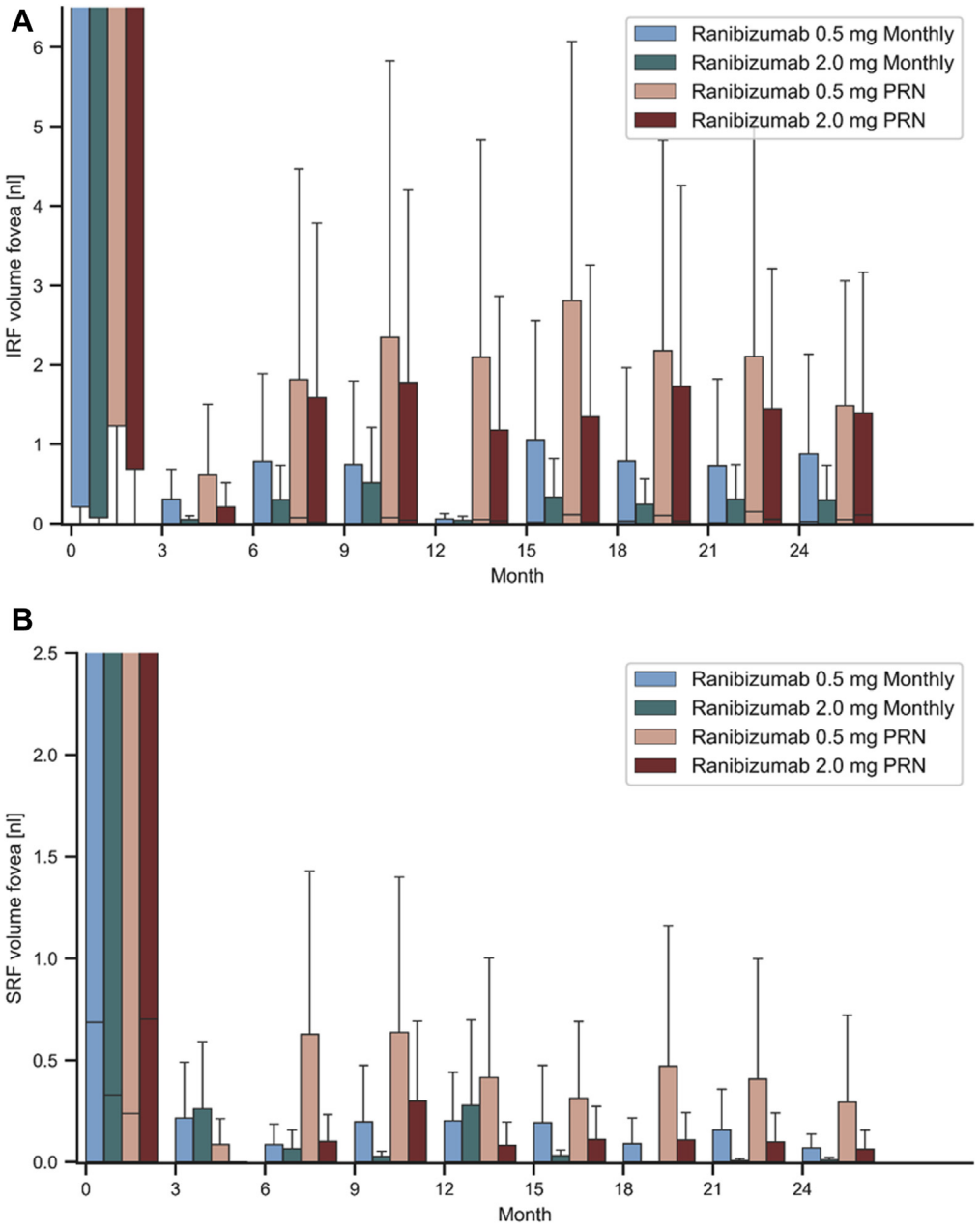

Figure 4. Box plots showing the distribution of fluid volumes in the central 1 mm (fovea) over time and for each treatment arm for **(A)** intraretinal fluid (IRF) and **(B)** subretinal fluid (SRF). PRN = pro re nata.

decrease in PED volumes even with a monthly regimen. The long-term persistence of PED possibly reflects the conversion from a serous to fibrovascular RPE detachment. Because of the primary choriocapillary origin of the neovascular complex, anatomic PED boundaries measured in a volumetric manner may objectively reflect the condition of the CNV, with PED enlargement predicting fluid recurrence, as reported by Penha et al.[38]

The conclusions of our fluid measurements in the 3 compartments of 1095 eyes/24 362 OCT volumes/more than 3 mio B-scans with monthly follow-up are important in the following ways. (1) We show that fluid resolution differs between different treatment arms in a volumetric manner. (2) A realistic relationship per unit volume (100 nl) of different fluid compartments with BCVA for a population with neovascular AMD is presented and may replace CRT as a parameter not related to BCVA. (3) We confirm on a metric level IRF (volume) as the major factor impacting function corresponding to its quantity. The multicystic distribution of IRF cannot be evaluated precisely without the use of a pixel-based automated segmentation. (4) The SRF was detected and accurately measured, and SRF pooling was detected mostly beyond the central mm as a result of a reliable localization. (5) The

A

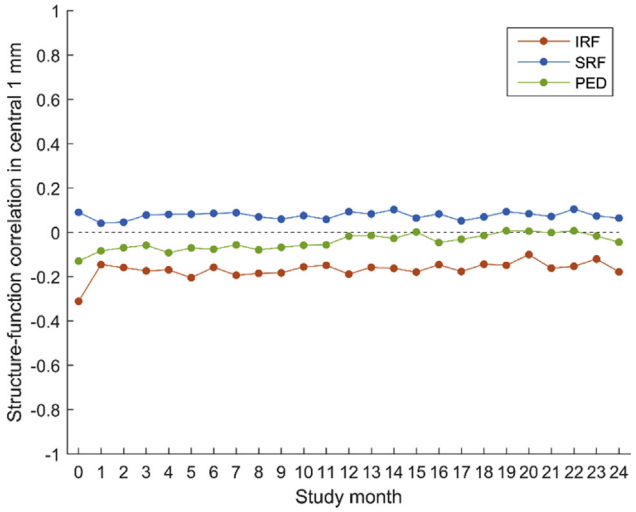

B

Fluid type	ΔBCVA	p-value
IRF in central 1 mm	-4.00 (-4.44 / -3.55)	p < 0.0001
SRF in central 1 mm	+1.10 (+0.34 / 1.86)	p = 0.0046
PED in central 1 mm	-0.35 (-0.57 / -0.13)	p = 0.0021
R^2 (marginal/conditional)	0.025/ 0.924	

Figure 5. A, Trajectories of structure-function correlation per compartment over time pooled over the 4 treatment arms. Structure is represented by measured fluid volumes of intraretinal fluid (IRF), subretinal fluid (SRF), and pigment epithelial detachment (PED) in the central 1 mm. **B,** Result of multivariable mixed effect modeling indicating the association between an increase of 100 nl (=0.1 mm^3) of fluid and associated change in best-corrected visual acuity (BCVA) for each fluid type.

poor correlation of reading center and clinicians' evaluation, in respect to IRF,[28] using a purely qualitative approach or yes/no presence demonstrates the need for a reliable quantitative volume segmentation. The novelty and purpose of this article are in the clinical observations obtained from the application of the novel quantitative method on such a large data set of patients undergoing anti-VEGF treatment with different regimens and dosages and proof-of-principle that the measured fluid volumes indeed correspond so tightly to the therapeutic conditions. Obviously, as re-treatment decisions were by protocol based on the qualitative presence of fluid, the fact that treatment was done does not mean that treatment was needed. Quantitative correlations together with differentiation of fluid types may now allow identification of BCVA-relevant re-treatment parameters and improve outcomes with less re-treatment need.

Automated quantification of fluid response may improve the therapeutic management of neovascular AMD, avoid discrepancies between clinicians/investigators, and establish a structure/function correlation, potentially led by IRF quantification. Prospective clinical studies will have to be performed to provide future evidence of such a point-of-care concept.

In image-guided diagnosis and therapy, AI has already delivered breakthroughs in fields such as radiology and dermatology. The approval of a fully automated method for the detection of diabetic retinopathy by the Food and Drug Administration and European Medicines Agency in 2018 marked a milestone in ophthalmology.[39] Spectral-domain OCT imaging is already important for disease management. Between 2008 and 2015, US healthcare accrued savings of an estimated 10 billion USD by the use of OCT.[40] The potential for further optimization by advanced AI-based autonomous analyses is exciting. If confirmed in prospective trials, the introduction of AI-based algorithms may allow the retinologist everywhere in the world to detect, localize, and quantify fluid in a fast, reliable, and automated manner. The transition from qualitative OCT assessment with all its real-world deficiencies to a reliable quantification may result in a paradigm shift in macular disease management. The FLUID study has recently suggested an IRF-focused therapy while tolerating SRF.[41] Such concepts have to be consolidated before being introduced in clinical routine, particularly because central SRF height does not correlate with overall SRF volume.

In conclusion, the treatment of the right patient at the right time with the right regimen is clearly a goal for physicians, patients, and healthcare providers. Artificial intelligence—based evaluations predicting outcomes and therapeutic requirements may also optimize the use of resources.[42,43] Unsupervised methods of deep learning could change our understanding of the pathogenesis of AMD by eliminating previous bias in biomarker search.[44]

References

1. Vos T, Allen C, Arora M, et al. Global, regional, and national incidence, prevalence, and years lived with disability for 310 diseases and injuries, 1990-2015: a systematic analysis for the Global Burden of Disease Study 2015. *Lancet*. 2016;388:1545−1602.
2. Jager RD, Mieler WF, Miller JW. Age-related macular degeneration. *N Engl J Med*. 2008;358:2606−2617.
3. Spaide RF, Fujimoto JG, Waheed NK, et al. Optical coherence tomography angiography. *Prog Retin Eye Res*. 2018;64:1−55.
4. Daniel E, Toth CA, Grunwald JE, et al. Risk of scar in the comparison of age-related macular degeneration treatments trials. *Ophthalmology*. 2014;121:656−666.
5. Rosenfeld PJ, Brown DM, Heier JS, et al. Ranibizumab for neovascular age-related macular degeneration. *N Engl J Med*. 2006;355:1419−1431.
6. Windsor MA, Sun SJJ, Frick KD, et al. Estimating public and patient savings from basic research-a study of optical coherence tomography in managing antiangiogenic therapy. *Am J Ophthalmol*. 2018;185:115−122.
7. Group CR, Martin DF, Maguire MG, et al. Ranibizumab and bevacizumab for neovascular age-related macular degeneration. *N Engl J Med*. 2011;364:1897−1908.
8. Martin DF, Maguire MG, Fine SL, et al. Ranibizumab and bevacizumab for treatment of neovascular age-related macular degeneration: two-year results. *Ophthalmology*. 2012;119:1388−1398.
9. Sharma S, Toth CA, Daniel E, et al. Macular morphology and visual acuity in the second year of the Comparison of Age-Related Macular Degeneration Treatments Trials. *Ophthalmology*. 2016;123:865−875.
10. Mehta H, Tufail A, Daien V, et al. Real-world outcomes in patients with neovascular age-related macular degeneration treated with intravitreal vascular endothelial growth factor inhibitors. *Prog Retin Eye Res*. 2018;65:127−146.
11. Obermeyer Z, Emanuel EJ. Predicting the future - big data, machine learning, and clinical medicine. *N Engl J Med*. 2016;375:1216−1219.
12. Schmidt-Erfurth U, Sadeghipour A, Gerendas BS, et al. Artificial intelligence in retina. *Prog Retin Eye Res*. 2018;67:1−29.
13. Schlegl T, Waldstein SM, Bogunovic H, et al. Fully automated detection and quantification of macular fluid in OCT using deep learning. *Ophthalmology*. 2018;125:549−558.
14. Ho AC, Busbee BG, Regillo CD, et al. Twenty-four-month efficacy and safety of 0.5 mg or 2.0 mg ranibizumab in patients with subfoveal neovascular age-related macular degeneration. *Ophthalmology*. 2014;121:2181−2192.
15. Zhang L, Sonka M, Folk JC, et al. Quantifying disrupted outer retinal-subretinal layer in SD-OCT images in choroidal neovascularization. *Invest Ophthalmol Vis Sci*. 2014;55:2329−2335.
16. Garvin MK, Abramoff MD, Wu X, et al. Automated 3-D intraretinal layer segmentation of macular spectral-domain optical coherence tomography images. *IEEE Trans Med Imaging*. 2009;28:1436−1447.
17. Ritter M, Elledge J, Simader C, et al. Evaluation of optical coherence tomography findings in age-related macular degeneration: a reproducibility study of two independent reading centres. *Br J Ophthalmol*. 2011;95:381−385.
18. Simader C, Ritter M, Bolz M, et al. Morphologic parameters relevant for visual outcome during anti-angiogenic therapy of neovascular age-related macular degeneration. *Ophthalmology*. 2014;121:1237−1245.
19. Schmidt-Erfurth U, Waldstein SM, Deak GG, et al. Pigment epithelial detachment followed by retinal cystoid degeneration leads to vision loss in treatment of neovascular age-related macular degeneration. *Ophthalmology*. 2015;122:822−832.
20. Vogl WD, Waldstein SM, Gerendas BS, et al. Analyzing and predicting visual acuity outcomes of anti-VEGF therapy by a longitudinal mixed effects model of imaging and clinical data. *Invest Ophthalmol Vis Sci*. 2017;58:4173−4181.
21. Johnson PC. Extension of Nakagawa & Schielzeth's R(2) GLMM to random slopes models. *Methods Ecol Evol*. 2014;5:944−946.
22. Bates D, Mächler M, Bolker B, Walker S. Fitting linear mixed-effects models using lme4. *J Stat Softw*. 2015;67:1−48.
23. Rosenfeld PJ. Optical coherence tomography and the development of antiangiogenic therapies in neovascular age-related macular degeneration. *Invest Ophthalmol Vis Sci*. 2016;57:14−26.
24. Busbee BG, Ho AC, Brown DM, et al. Twelve-month efficacy and safety of 0.5 mg or 2.0 mg ranibizumab in patients with subfoveal neovascular age-related macular degeneration. *Ophthalmology*. 2013;120:1046−1056.
25. Hykin P, Chakravarthy U, Lotery A, et al. A retrospective study of the real-life utilization and effectiveness of ranibizumab therapy for neovascular age-related macular degeneration in the UK. *Clin Ophthalmol*. 2016;10:87−96.
26. Vaze A, Fraser-Bell S, Gillies M. Consequences of long-term discontinuation of vascular endothelial growth factor inhibitor therapy in the patients with neovascular age-related macular degeneration. *Acta Ophthalmol*. 2014;92:e697−698.
27. Lowry EA, Nguyen V, Daien V, et al. Outcomes in neovascular age-related macular degeneration when neovascular lesion activity is uncertain: observational study. *Ophthalmol Retina*. 2018;2:531−538.
28. Toth CA, Decroos FC, Ying GS, et al. Identification of fluid on optical coherence tomography by treating ophthalmologists versus a reading center in the Comparison of Age-Related Macular Degeneration Treatments Trials. *Retina*. 2015;35:1303−1314.
29. Gulshan V, Peng L, Coram M, et al. Development and validation of a deep learning algorithm for detection of diabetic retinopathy in retinal fundus photographs. *JAMA*. 2016;316:2402−2410.
30. Tolentino MJ, Miller JW, Gragoudas ES, et al. Intravitreous injections of vascular endothelial growth factor produce retinal ischemia and microangiopathy in an adult primate. *Ophthalmology*. 1996;103:1820−1828.
31. Wickremasinghe SS, Sandhu SS, Busija L, et al. Predictors of AMD treatment response. *Ophthalmology*. 2012;119:2413−2414 e5.
32. Kodjikian L, Decullier E, Souied EH, et al. Predictors of one-year visual outcomes after anti-vascular endothelial growth factor treatment for neovascular age-related macular degeneration. *Retina*. 2018;38:1492−1499.
33. Waldstein SM, Philip AM, Leitner R, et al. Correlation of 3-dimensionally quantified intraretinal and subretinal fluid with visual acuity in neovascular age-related macular degeneration. *JAMA Ophthalmol*. 2016;134:182−190.
34. Jaffe GJ, Martin DF, Toth CA, et al. Macular morphology and visual acuity in the comparison of age-related macular degeneration treatments trials. *Ophthalmology*. 2013;120:1860−1870.
35. Grunwald JE, Daniel E, Huang J, et al. Risk of geographic atrophy in the comparison of age-related macular degeneration treatments trials. *Ophthalmology*. 2014;121:150−161.
36. Klimscha S, Waldstein SM, Schlegl T, et al. Spatial correspondence between intraretinal fluid, subretinal fluid, and

pigment epithelial detachment in neovascular age-related macular degeneration. *Invest Ophthalmol Vis Sci*. 2017;58:4039–4048.
37. Schmidt-Erfurth U, Kaiser PK, Korobelnik JF, et al. Intravitreal aflibercept injection for neovascular age-related macular degeneration: ninety-six-week results of the VIEW studies. *Ophthalmology*. 2014;121:193–201.
38. Penha FM, Gregori G, Garcia Filho CA, et al. Quantitative changes in retinal pigment epithelial detachments as a predictor for retreatment with anti-VEGF therapy. *Retina*. 2013;33:459–466.
39. Abramoff MD, Folk JC, Han DP, et al. Automated analysis of retinal images for detection of referable diabetic retinopathy. *JAMA Ophthalmol*. 2013;131:351–357.
40. Rosenfeld PJ, Windsor MA, Feuer WJ, et al. Estimating Medicare and patient savings from the use of bevacizumab for the treatment of exudative age-related macular degeneration. *Am J Ophthalmol*. 2018;191:135–139.
41. Guymer RH, Markey CM, McAllister IL, et al. Tolerating subretinal fluid in neovascular age-related macular degeneration treated with ranibizumab using a treat-and-extend regimen: FLUID Study 24-month results. *Ophthalmology*. 2019;126:723–734.
42. Bogunovic H, Waldstein SM, Schlegl T, et al. Prediction of anti-VEGF treatment requirements in neovascular AMD using a machine learning approach. *Invest Ophthalmol Vis Sci*. 2017;58:3240–3248.
43. De Fauw J, Ledsam JR, Romera-Paredes B, et al. Clinically applicable deep learning for diagnosis and referral in retinal disease. *Nat Med*. 2018;24:1342–1350.
44. Seebock P, Waldstein SM, Klimscha S, et al. Unsupervised identification of disease marker candidates in retinal OCT imaging data. *IEEE Trans Med Imaging*. 2019;38:1037–1047.

Footnotes and Financial Disclosures

Originally received: July 11, 2019.
Final revision: March 2, 2020.
Accepted: March 4, 2020.
Available online: March 16, 2020. Manuscript no. 2019-1523.

[1] Christian Doppler Laboratory for Ophthalmic Image Analysis, Department of Ophthalmology and Optometry, Medical University of Vienna, Vienna, Austria.

[2] Department of Ophthalmology, Feinberg School of Medicine, Northwestern University, Chicago, Illinois.

Financial Disclosure(s):
The author(s) have made the following disclosure(s): U.S.-E.: Consultant – Boehringer Ingelheim, Genentech, Novartis, and Roche. The other authors do not have any conflicts to disclose.

Supported by the Austrian Federal Ministry for Digital and Economic Affairs.

HUMAN SUBJECTS: Human subjects were included in this study. The human ethics committees at the Medical University of Vienna approved the study. All research adhered to the tenets of the Declaration of Helsinki. All participants provided informed consent at the respective centers before enrollment into the HARBOR clinical trial.

No animal subjects were used in this study.

Author Contributions:

Conception and design: Schmidt-Erfurth

Data collection: Vogl, Bogunović

Analysis and interpretation: Schmidt-Erfurth, Vogl, Jampol, Bogunović

Obtained funding: Schmidt-Erfurth

Overall responsibility: Schmidt-Erfurth, Vogl, Jampol, Bogunović

Abbreviations and Acronyms:
AI = artificial intelligence; **AMD** = age-related macular degeneration; **BCVA** = best-corrected visual acuity; **CNN** = convolutional neural network; **CRT** = central retinal thickness; **IRF** = intraretinal fluid; **PED** = pigment epithelial detachment; **PRN** = pro re nata; **RPE** = retinal pigment epithelium; **SD** = spectral domain; **SRF** = subretinal fluid; **VEGF** = vascular endothelial growth factor.

Correspondence:
Ursula Schmidt-Erfurth, MD, Department of Ophthalmology and Optometry, Medical University of Vienna, Spitalgasse 23, 1090 Vienna, Austria. E-mail: ursula.schmidt-erfurth@meduniwien.ac.at.